Taming the Dichalcogenides: Isolation, Characterization, and Reactivity of Elusive Perselenide, Persulfide, Thioselenide, and Selenosulfide Anions

Keyan Li, Lev N. Zakharov, and Michael D. Pluth*

Department of Chemistry and Biochemistry, Materials Science Institute, Knight Campus for Accelerating Scientific Impact, and Institute of Molecular Biology, University of Oregon, Eugene, Oregon, 97403-1253, United States.

* pluth@uoregon.edu

Abstract

Reactive sulfur species (RSS) and reactive selenium species (RSeS) play integral roles in hydrogen sulfide (H_2S) and hydrogen selenide (H_2Se) biological signaling pathways, and dichalcogenide anions are proposed transient intermediates that facilitate a variety of biochemical transformations. Herein we report the selective synthesis, isolation, spectroscopic and structural characterization, and fundamental reactivity of persulfide (RSS⁻), perselenide (RSeSe⁻), thioselenide (RSSe⁻), and selenosulfide (RSeS⁻) anions. The isolated chalcogenides do not rely on steric protection for stability and have steric profiles analogous to cysteine (Cys). Simple reduction of S_8 or Se by potassium benzyl thiolate (KSBn) or selenolate (KSeBn) in the presence of 18-crown-6 afforded [K(18-crown-6)][BnSS] (**1**), [K(18-crown-6)][BnSeSe] (**2**) [K(18-crown-6][BnSSe] (**3**), and [K(18-crown-6][BnSeS] (**4**). The chemical structure of each dichalcogenide was confirmed by X-ray crystallography and solution state ^1H, ^{13}C, and ^{77}Se NMR spectroscopy. To advance our understanding of the reactivity of these species, we demonstrated that reduction of **1-4** by PPh₃ readily generates E=PPh₃ (E: S, Se), and reduction of **1**, **3**, and **4** by DTT readily produces HE⁻/H_2E. Furthermore, **1-4** reacts with CN⁻ to produce ECN⁻, which is consistent with the detoxifying effects of dichalcogenide intermediates in the Rhodanese enzyme. Taken together, this work provides new insights into the inherent structural and reactivity characteristics of dichalcogenides relevant to biology and advances our understanding of the fundamental properties of these reactive anions.
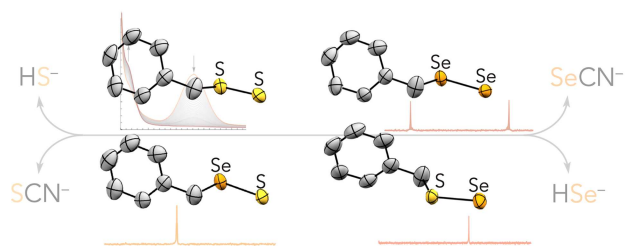
Introduction

Endogenously produced small gaseous molecules are essential and facilitate of a wide array of physiological processes. For example, hydrogen sulfide (H_2S), nitric oxide ($NO^{\bullet}$) and carbon monoxide (CO) are all established gasotransmitters that play active and expanding roles in complex biological processes such as neural transduction, angiogenesis, and vasodilation.[1, 2] More recently, hydrogen selenide (H_2Se) has emerged as a potential new addition to this group due to its integral role in mammalian selenium homeostasis, antioxidant enzyme activity, thyroid functions, and other processes – all of which make selenium an essential bioinorganic element the human diet.[3-5] This growing biological significance has catalyzed the recent development of chemical tools for delivery and detection of H_2Se in biology[6-13] and also raised questions about the fundamental reactivity differences of reactive sulfur and selenium species (RSS and RSeS).

The broad utilization of S and Se by Nature is likely due to their versatile redox chemistry with biologically accessible oxidation states spanning from –2 to +6. This redox availability enables the generation of a diverse array of complex and intertwined reactive RSS and RSeS crucial in cellular signaling.[14-16] Established RSS and RSeS typically contain S and Se in the –2 to 0 oxidation states, which provides a duality to these species to act as either pro- or anti-oxidants. Key RSS examples include H_2S/HS^-, thiols (RSH), persulfides (RSS^-), and organic/inorganic polysulfides ($R_2S_{n>2}$, HSS_n^-), whereas analogous examples of RSeS include H_2Se/HSe^-, selenols (RSeH), thioselenides ($RSSe^-$), and selenotrisulfides (RSSeSR).[14, 17] Although S and Se are often considered two of the most similar elements on the periodic table, a number of enzymes rely on Se rather than S for key active site transformations. For example, formate dehydrogenase (FDH), glycine reductase (Grd), and glutathione peroxidase (Gpx) all carry out typically energy intensive transformations and benefit from the enhanced nucleophilicity, better leaving group ability, and lower redox potential of Se over S.[18, 19]

Dichalcogenides highlight the intersection of RSS and RSeS with persulfides (RSS^-), thioselenides ($RSSe^-$), and selenosulfides ($RSeS^-$) being proposed intermediates in numerous biochemical processes, whereas perselenides ($RSeSe^-$) have remained primarily a yet-uncharacterized chemical curiosity. RSS^- are the most established dichalcogenides, and glutathione persulfide anion (GSS^-) and cysteine persulfide anion ($CysSS^-$) are both readily

3

generated under physiological conditions.[20, 21] Critical biological roles of RSS⁻ include the construction of iron-sulfur (Fe-S) clusters by the protein scaffold ISCU,[22] detoxification of cyanide (CN⁻) by the Rhodanese enzyme (RhdA),[23-25] and mammalian production of H_2S by 3-mercaptopyruvate sulfurtransferase (3-MST).[20, 26] As for the more fleeting RSSe⁻, both glutathione thioselenide (GSSe⁻) and enzyme-bound thioselenide (Enz-SSe⁻) have been postulated as highly reactive intermediates in RhdA prior to reduction to HSe⁻ or selenophosphate generation.[27] In contrast, the isomeric RSeS⁻ has been observed crystallographically as a Ni-bound selenocysteine selenosulfide (SecSeS⁻) in the active site of [NiFeSe] hydrogenase from *Desulfovibrio vulgaris*, which generates hydrosulfide (HS⁻) upon reduction.[28] Similarly, a Mo-bound SecSeS⁻ is a proposed intermediate in the catalytic oxidation of formate by Mo FDH.[29] Finally, RSeSe⁻ motifs have thus far remained both biologically and chemically elusive, which is likely further confounded the expected high chemical reactivity of this functional group as well as the trace levels of Se required for biological function. We note that given the rarity and elusiveness of such motifs, the term "perselenide" has been used sporadically in the literature to describe the heterodichalcogenide RSSe⁻ (thioselenide) rather than the more accurate RSeSe⁻ formulation.
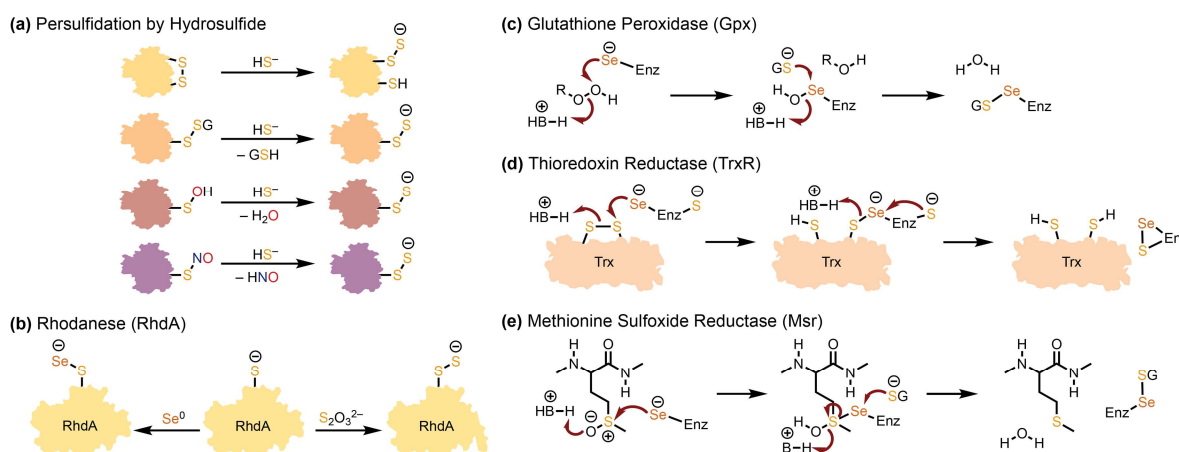

Figure 1. Selected biological pathways for S–S and Se–S bond formation. (a) Persulfidation at oxidized protein thiols, (b) formation of RhdA-bound RSS⁻ and RSSe⁻, (c) proposed S–Se bond formation by glutathione peroxidase, (d) thioredoxin reductase, and (e) methionine sulfoxide reductase (Enz–Se⁻: enzyme-bound selenocysteine selenolate; GS⁻: glutathione thiolate; Trx: thioredoxin; B⁺–H: proton source.) This figure is adapted in part from Ref. (15,16)

In general, biosynthetic pathways resulting in dichalcogenide formation typically involve the reduction of a partially oxidized S/Se (o.s. $\geq$–1) by a fully reduced (o.s = –2) S/Se. For RSS^- generation (persulfidation), the reduction of an oxidized protein thiol (e.g. cysteine disulfide, glutathiolated cysteine, cysteine sulfenic acid, or S-nitroso cysteine) by HS^- generates a persulfide, which predominantly exist as RSS^- at physiological pH due to the increased persulfide acidity (pK_a ≈ 6.2) (Figure 1a).[16, 21] Alternatively, protein-bound $CysS^-$ in RhdA can reduce the S^0 of thiosulfate ($S_2O_3^{2-}$) to form $CysSS^-$.[23, 24] Persulfidation-like pathways have also been proposed for $RSSe^-$ generation, in which HSe^- reduces oxidized protein thiols to generate $RSSe^-$.[8] Alternatively, glutathione thiolates (GS^-) can reduce oxidized Se to form $GSSe^-$ in RhdA (Figure 1b).[27] Similar reduction of oxidized Se by GS^- has also been proposed in both glutathione peroxidase (Gpx) and methionine sulfoxide reductase (Msr), where enzyme-bound GS-Se-Enz intermediates are likely generated (Figure 1c). Although prior pathways detailing $RSeS^-$ formation are limited, the reduced selenide (Enz-Sec-Se$^-$) in thioredoxin reductase (TrxR) can reduce the disulfide bridge of thioredoxin to form enzyme-bound Enz-Sec-Se-S intermediates, suggesting that highly nucleophilic selenolate selenocysteine (Sec$^-$) can reduce sulfane sulfur (S^0) to produce $SecSeS^-$ (Figure 1d-1e).[15]

Despite the recognized importance and potential biological roles of these anionic dichalcogenides, the fundamental chemistry of such anions remains essentially unexplored. Our group previously reported the isolation and characterization of the sterically encumbered trityl hydropersulfide (TrtSSH, Trt = Ph_3C), but our prior attempt to access $TrtSS^-$ through deprotonation led to immediate disproportionation to form TrtSH and S_8.[30] Similarly, Nakayama and co-workers have attempted deprotonation of a triptycene-substituted hydroselenosulfide (TrpSeSH), resulting only formation of undesirable decomposition products rather than $TrpSeS^-$.[31] Although a Zn-bound $TrtSS^-$ was reported by Artaud and co-workers,[32] the only structurally characterized noncovalently-bound RSS^- examples were reported by groups of Rauchfuss and Chen, where reduction of S_8 by PhS^- or $tBuS^-$ provided $PhSS^-$ and $tBuSS^-$, respectively.[33, 34] Despite the resonance stabilization from the adjacent Ph substituent in $PhSS^-$ and steric bulk in $tBuSS^-$, the S–S bonds in both species are highly labile in solution and form higher order polysulfides RSS_n^- or the highly colored radical anion $S_3^{\bullet-}$ even at low temperatures. Such complex

solution equilibria present further complications in elucidating the reactivities of RSS⁻. In the above cases, the need for steric protection of the persulfide motif was heavily emphasized and attempts to use less sterically bulky analogues with methylene groups adjacent to the dichalcogenide, such as in CysS⁻, have proven unsuccessful. Highlighting this heightened reactivity, structural characterization of a free RSSe⁻ species was only reported recently by Chen and coworkers, in which a reaction between NaSPh and Se in the presence of [PPh₄][Cl] furnished a mixture of [PPh₄][PhSSe] and trace amounts of the accompanying polyselenide [PPh₄]₂[Se₅].[35] Similar to PhSS⁻, PhSSe⁻ also exhibits complex in-solution equilibria even at low temperatures as evidenced by NMR spectroscopy. Further reactivity of this motif was not investigated. To the best of our knowledge, RSeS⁻ and RSeSe⁻ motifs have not yet been structurally characterized, although the related perselenanyl radical (RSeSe•) was recently reported by Stalke and co-workers by photolysis of Bn₂Se₂ in the solid-state.[36]

Given the biological relevance of these understudied dichalcogenide motifs, we viewed that the direct characterization of RSSe⁻, RSeS⁻, RSS⁻, and RSeSe⁻ compounds would provide a useful platform for not only structural characterization but also for probing initial reactivity. Moreover, understanding the chemical reactivity of these compounds could also provide new synthetic strategies to access established H₂S releasing scaffolds such as functionalized selenylsulfides (RSSeR′), thioselenic acids (RSeSH), and hydropersulfides (RSSH).[37] Although prior strategies to stabilize highly reactive S and Se species have often relied on sterically protected substituents, [30, 31, 38, 39] our approach here the uses contact ion pairing interactions with complexed alkali metal cations, such as [K(18-crown-6)]⁺ and [Na(15-crown-5)]⁺, which has previously enabled the isolation of various reactive anions.[40-42] Using this approach, we herein report the syntheses, isolation, characterization, and comparative reactivities of structurally simple RSS⁻, RSeSe⁻, RSSe⁻, and RSeS⁻ dichalcogenides.

Syntheses and Characterizations

Building from the hypothesis that contact ion pairing could help stabilize anionic dichalcogenides, we treated THF solutions of [K(18-crown-6)][BnS] or [K(18-crown-6)][BnSe] generated *in situ* with ¹/₈ equiv. of S₈ or 1 equiv. of solid gray Se powder (Scheme 1). These reaction conditions provided the dichalcogenides [K(18-crown-6)][BnSS] (**1**), [K(18-crown-

6)][BnSeSe] (**2**) [K(18-crown-6][BnSSe] (**3**), and [K(18-crown-6][BnSeS] (**4**), which were characterized by NMR spectroscopy, UV-vis spectroscopy, and X-ray crystallography. The ^{1}H NMR spectra of **1-4** in CD$_3$CN were well-resolved at room temperature, and no fast exchange or paramagnetic broadening was observed. This stability is contrary to the observation by Chen and coworkers on the solution dynamics of [PPh$_4$][PhSSe], which further supports that the typically labile dichalcogenide bonds in **1-4** remain intact in solution despite the absence of steric or resonance stabilization. In general, **1-4** are stable in the solid state when stored under an inert atmosphere. Multiple attempts to obtain mass spectrometric characterization for **1**, **2** and **4** proved unsuccessful, indicating their instability upon ionization, particularly in the gas phase. In solution, the terminal Se containing **2** and **3** exhibit remarkable stability in MeCN, whereas the terminal S containing **1** and **4** undergo gradual decomposition in solution to form polysulfides and various other decomposition products over the course of a few days.

Scheme 1. Synthesis of dichalcogenides 1–4. (E = S, Se)

1: E$_\beta$ = S, E$_\alpha$ = S
2: E$_\beta$ = Se, E$_\alpha$ = Se
3: E$_\beta$ = S, E$_\alpha$ = Se
4: E$_\beta$ = Se, E$_\alpha$ = S
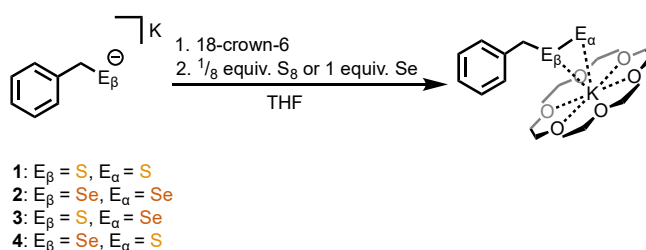
The ^{1}H NMR spectra of **1-4** display high sensitivity of the benzyl methylene protons to the nearby electronic environments of the dichalcogenide motif. As anticipated, the benzyl proton resonances are shifted more upshifted for the S-alkylated anions **1** (3.49 ppm) and **3** (3.57 ppm) than for the Se-alkylated anions **2** (3.66 ppm) and **4** (3.61 ppm). We also used ^{77}Se NMR spectroscopy to further probe the Se electronic environment in **2-4**. For perselenide **2**, the ^{77}Se NMR spectrum revealed two resonances at 170.9 ppm and 225.6 ppm corresponding to the terminal (E$_\alpha$) and internal selenides (E$_\beta$) Se atoms, respectively. These peaks are slightly broadened due to unresolved Se-Se and CH$_2$-Se couplings. For thioselenide **3**, a sharp singlet at 306.2 ppm was observed. This drastic downfield shift when compared to **2** is consistent with our hypothesis that substitution of S for Se at the E$_\beta$ position should generate a more electron-deficient terminal selenide due to the electronegativity difference between S and Se. Similar differences are observed

for the ^{77}Se NMR chemical shifts for the E$_\beta$ positions with the ^{77}Se NMR spectrum of selenosulfide **4** showing a sharp triplet at 318.2 ppm, which is shifted downfield by nearly 100 ppm when compared to **2** (Figure 2).
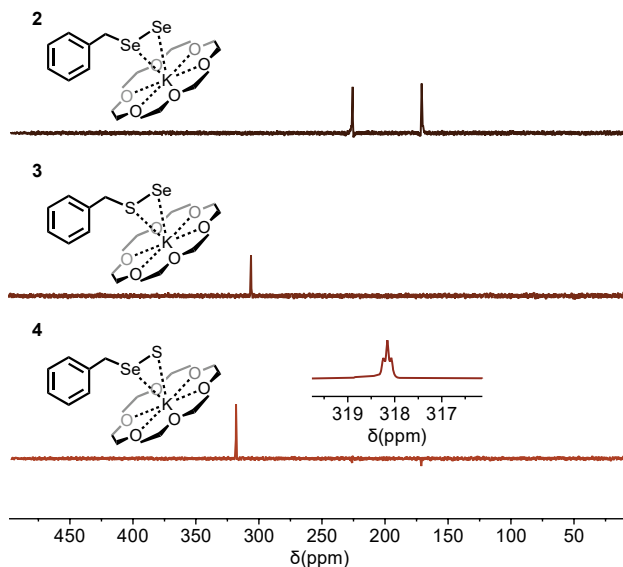

Figure 2. ^{77}Se NMR spectra of **2** (top), **3** (middle), and **4** (bottom) acquired in CD$_3$CN at 233 K.

The UV-Vis spectra of **1-4** all show features with moderate bathochromic shifts in the nb→σ* absorbance with increasing selenium substitution (λ_{max}(**1**): 373 nm, λ_{max}(**2**): 453 nm, λ_{max}(**3**): 418 nm, λ_{max}(**4**): 410 nm). Similar extinction coefficients were observed for compounds **2** and **3** with Se atoms in the E$_\alpha$ position and between compounds **1** and **4** with S atoms in the E$_\alpha$ position (Figure 3a). For selenosulfide **4**, however, the UV-Vis spectrum revealed a weak and unexpected absorbance at 610 nm, which we attribute to the radical anion S$_3^{\bullet-}$ formed through equilibrium of **4** with Bn$_2$Se$_2$ and inorganic polysulfides. Consistent with this hypothesis, our initial efforts to crystalize **4** led to the formation and isolation of the stable polysulfide anion [K(18-crown-6)]$_2$[S$_4$], which was isolated and characterized by X-ray crystallography. Further supporting the intermediacy of polysulfide anions in dichalcogenide formation, monitoring the UV-Vis spectrum of KSBn treated with S$_8$ shows a transient absorbance at 610 nm corresponding to S$_3^{\bullet-}$ formation, which bleaches completely upon formation of stable persulfide **1** (Figure 3b).
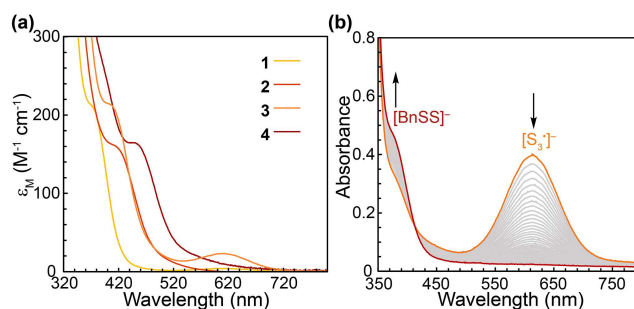
Figure 3. (a) UV-vis spectra of **1-4** in (solvent) acquired at room temperature. (b) UV-Vis trace of the reaction between KSBn and S_8, which shows the diminishing absorbance of $S_3^{\bullet-}$ (λ_{max}=610 nm) and the emergence of n.b. to σ^* transition corresponding to **1** (λ_{max}=373 nm). Spectra were acquired every 2 minutes.

Structural Analysis

We also characterized dichalcogenides **1-4** by X-ray crystallography to confirm our structural assignments and also to better understand structural differences between these reactive anions (Figure 4). Crystals of **1-4** suitable for X-ray diffraction studies were grown by layering of Et_2O onto a saturated solution of **1** in MeCN or by vapor diffusion of Et_2O into saturated solution of **2-4** in MeCN. The S–S distance in **1** is 2.053(2) Å, which is longer than the S–S distances in resonance stabilized [PhSS][PPh_4] (2.043(11) Å) and shorter than in sterically encumbered [*t*BuSS][PPh_4] (2.067(6) Å).[34] The S–S distance in **1** is also shorter than the shortest S–S distance in the dianion [K(18-crown-6)]$_2$[S_4] (of 2.049(8) Å), which has additional stabilization from two [K(18-crown-6)]$^+$ contact ion pairs.[40] The S–S bond in **1** is longer than neutral S_2-containing species, such as Bn_2S_2 (2.037(5) Å) and TrtSSH (2.039(12) Å).[30, 43] This elongated bond distance is consistent with increased electron density in the S–S nonbonding orbital, which promotes destabilizing interactions between the lone pairs. In addition, strong contact-ion pairing interactions are observed between the S–S unit and [K(18-crown-6)]$^+$ as evidenced by the short distances between the terminal (S_α) and internal (S_β) sulfur atoms and the K atom of 3.624(1) and 3.089(2) Å, respectively. The S_β–S_α–K angle of 87.18(6)º also supports that [K(18-crown-6)]$^+$ is interacting with S_α–S_β unit rather than just the terminal S_α atom.

The Se–Se bond distance of perselenide **2** is 2.322(1)Å, which is significantly longer than the S–S bond in **1** as expected. The Se–Se bond distance in **2** is also longer than that in Bn_2Se_2 (2.315 Å) and $BnSeSe^\bullet$ (2.243 Å),[30] which is consistent with the enhanced lone pair repulsion in anionic **2**. The Se–Se distance of **2**, however, is shorter than in the related dianion [K(18-crown-6)]$_2$[Se$_4$] (2.332(1) Å).[41] Much like in the structure of **1**, the terminal (Se$_\alpha$) and internal (Se$_\beta$) selenium atoms both interact with the K atom, with relatively short Se$_\alpha$–K and Se$_\beta$–K distances of 3.215(2) and 3.875(2) Å, respectively. Both of these distances are longer than in **1**, which is consistent with the lower electronegativity of Se than S. Similar to the structure of **1**, the entire Se$_\alpha$–Se$_\beta$ unit appears to interact with the [K(18-crown-6)]$^+$ contact ion, with an Se$_\beta$–Se$_\alpha$–K angle of 87.26(5)º.
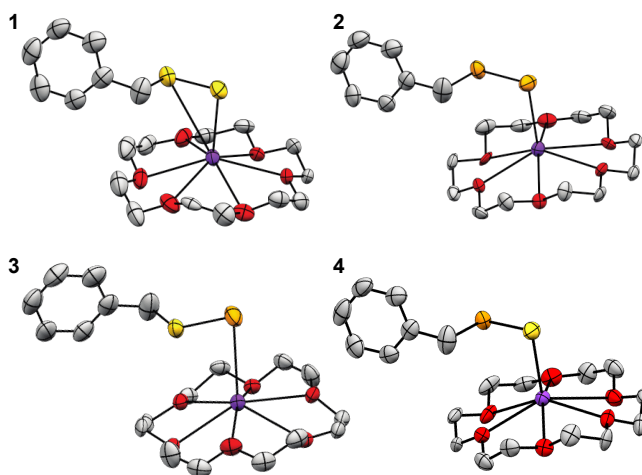

Figure 4. Solid-state structures of **1-4**. Purple, red, yellow, orange, and gray ellipsoids represent K, O, S, Se, and C atoms, respectively. Ellipsoids are shown at the 50% probability level. Solvent molecules and H atoms are omitted for clarity.

Moving to the heterodichalcogenides, thioselenide anion **3** has a S–Se bond distance of 2.214(2) Å, which is longer than the S–Se bond distances in resonance stabilized [PhSSe][PPh$_4$] of 2.1997(10) Å and for other structurally characterized neutral RSSeR species, which range from (2.125(3) - 2.201(4) Å).[35, 44-46] This bond elongation in **3** is consistent with the enhanced destabilizing lone-pair repulsion described above. Interactions between the terminal selenium

(Se$_\alpha$) and internal sulfur (S$_\beta$) atoms and the K atom are reflected in the short Se$_\alpha$–K and S$_\beta$–K distances of 3.206(1) Å and 3.798(2) Å, respectively. The Se$_\alpha$ and S$_\beta$ positions of **3** appear to interact more strongly with [K(18-crown-6)]$^+$ than in **2** but less strongly than in **1**, which matches the intermediate electron density of the S–Se motif when compared to the homodichalcogenides. Similar to the structures of **1** and **2**, the full Se$_\alpha$–S$_\beta$ unit interacts with the [K(18-crown-6)]$^+$ contact ion with a S$_\beta$–Se$_\alpha$–K angle of 86.96(4)º.

Lastly, selenosulfide anion **4** has a Se–S bond distance of 2.188(2) Å, which is longer than the Se–S bond in TrpSeSH (2.1796(9) Å) also the neutral RSSeR species described earlier.[26] Similar interactions between the terminal sulfur (S$_\alpha$) and internal selenium (S$_\beta$) atoms and the K atom are reflected in the short S$_\alpha$–K and Se$_\beta$–K distances of 3.115(3) and 3.728(2) Å, respectively. In addition, similar to the structure of **1**, the entire Se$_\alpha$–S$_\beta$ unit appears to interact with the [K(18-crown-6)]$^+$ contact ion as supported by the S$_\beta$–Se$_\alpha$–K angle of 87.52(7)º.

In addition to the stabilizing interactions offered by [K(18-crown-6)]$^+$, the contact ion interactions also allow for further insights into the electronic environments of E$_\alpha$ and E$_\beta$ positions in each dichalcogenide. Taking the ratio (R*) of bond distances (d) E$_\beta$–K and E$_\alpha$–K (R$^*= d_{E\beta K}/d_{E\alpha K}$) allows for direct comparison of E$_\beta$–K and E$_\alpha$–K interactions across structures of **1**-**4**. An R* value of 1 indicates equal E$_\beta$–K and E$_\alpha$–K interactions, and R*>1 values signify stronger interactions between K$^+$ and E$_\alpha$. Tabulation of R* values, as well as key structural parameters, are included in Table 1. The average R* across structures **1**-**4** is 1.190, which indicates that the α and β positions interact with K$^+$ almost equally with slight preference for the α position. When comparing homodichalcogenides **1** and **2**, perselenide **2** shows a greater R* value (1.205) than **1** (1.173), which is consistent with our hypothesis that Se$_\alpha$ is can better stabilized charge than S$_\alpha$ due to a more energetic accessible 4d orbital. The R* values of **1** and **2** are larger when compared to the related dianions [K(18-crown-6)]$_2$[S$_4$] (R$^*_{avg}$= 0.9661) and [K(18-crown-6)]$_2$[Se$_4$] (R$^*_{avg}$= 1.087), indicating that the α atoms of dichalcogenides bear significant more charge than in polychalcogenides. For heterodichalcogenides **3** and **4**, selenosulfide **4** has a larger R* value (1.197) than **3** (1.185), which is expected due to a more electronegative E$_\alpha$ atom in **4**.

Table 1. Selected structural parameters for 1-4 (E = S, Se).

	BnSS⁻ (1)	BnSeSe⁻ (2)	BnSSe⁻ (3)	BnSeS⁻ (4)
E_α–E_β (Å)	2.053(2)	2.322(1)	2.214(2)	2.188(2)
C1–E_β (Å)	1.836(6)	1.990(1)	1.846(8)	1.983(8)
E_α–K (Å)	3.089(2)	3.215(2)	3.206(1)	3.115(3)
E_β–K (Å)	3.624(1)	3.875(2)	3.798(2)	3.728(2)
C1–C2(Å)	1.503(9)	1.490(2)	1.497(1)	1.491(1)
$\angle E_\alpha E_\beta K$ (º)	87.18(6)	87.26(5)	86.96(4)	87.52(7)
R* (E_βK/E_αK)	1.173	1.205	1.185	1.197

Dichalcogenide Reactivity

Having structurally characterized dichalcogenides **1-4**, we next aimed to investigate the basic reactivity of these compounds toward simple reductants and electrophiles. Based on the role of RSS⁻ and RSSe⁻ as potential biological storage units for fully-reduced S^{2-} and Se^{2-} motifs, we first treated **1-4** with PPh₃ as a 2e⁻ reducing agent to determine whether fully reduced S/Se can be liberated. Furthermore, reduction with PPh₃ also allows for direct trapping of the fully reduced chalcogenide in the form of E=PPh₃ (E = S/Se), which can be readily observed by ¹H and ³¹P NMR spectroscopy. Reactions of **1** and **4** with PPh₃ led to the immediate reduction to KSBn and KSeBn, respectively, with generation of S=PPh₃ (δ(³¹P) = 42 ppm). Similarly, reduction of **2** and **3** showed analogous formation of the parent chalcogenates and Se=PPh₃ (δ(³¹P) = 35 ppm, $^1J_{P-Se}$ = 736 Hz) (Figure 5). Despite the simplicity of this reaction pathway, prior investigations with the neutral analogue of **1** (BnSSH) toward PPh₃ produced the organic polysulfide BnSSSBn and H₂S rather than the anticipated BnSH and S=PPh₃.[47] This reactivity difference between RSS⁻ and RSSH highlights the importance of protonation state in moderating persulfide reduction chemistry.
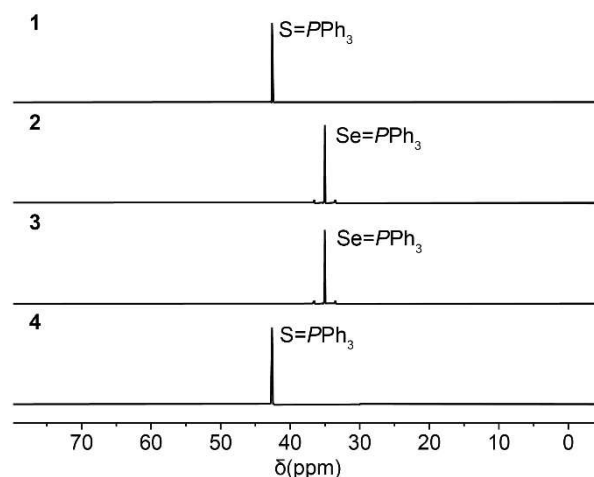
Figure 5. ^{31}P NMR spectra of reactions between **1-4** and PPh$_3$ to produce S=PPh$_3$ and Se=PPh$_3$.

The reduction of RSS$^-$ and RSSe$^-$ to form HS$^-$ and HSe$^-$ has been proposed in the biosyntheses of H$_2$S and H$_2$Se by 3-MST and RhdA, respectively. As proxies to this reactivity, we treated **1-4** first with dithiothreitol (DTT), which readily converted **1** to form thermodynamically favored cyclic disulfide and HS$^-$, which was trapped by BnBr as Bn$_2$S. Similarly, terminal sulfide-containing **4** is also rapidly reduced to form H$_2$S and BnSeK. Further treatment with PPh$_3$ failed to generate S=PPh$_3$, which confirmed the complete reduction of **1** and **4** by DTT. Similar reduction of thioselenide **3** with DTT forms HSe$^-$, as evidenced by a new peak in the ^{77}Se NMR spectrum at –426.5. We did not observe a direct reaction of perselenide **2** with DTT even in the presence of excess diisopropylamine. This observation suggests that generation of HSe$^-$ from **2** is not limited to its decreased basicity with increasing Se substitution. The reverse reaction, however, in which highly nucleophilic HSe$^-$ and BnSe$^-$ cooperatively reduce the cyclic disulfide, is likely favored in this scenario. Interestingly, the release of HS$^-$ and HSe$^-$ from **1-4** upon treatment with a reducing thiol differs from prior work with isolated neutral RSSH (R: Bn, Ad, Trt) in aprotic solvents, which do not react directly with thiols. This difference in reactivity between isolated RSSH and RSS$^-$ further highlights the important role of protonation states in mediating H$_2$S release and RSS reactivity.

Dichalcogenides are also hypothesized to play protective roles in RhdA-mediated detoxification of CN$^-$, and we investigated this reactivity directly by treating [NBu$_4$][CN] with **1-**

4 in CD$_3$CN. Addition of [NBu$_4$][CN] to persulfide **1** or selenosulfide **4** in CD$_3$CN did not result in an immediate reaction, but allowing the reaction mixture to stir overnight resulted in complete reduction of **1** and **4** to BnSK and BnSeK, respectively. IR spectra of the reaction products showed a strong stretch at 2054 cm^{-1} corresponding to thiocyanate (SCN$^-$) formation. This reactivity is consistent with the reported biological conversion of CN$^-$ to less toxic SCN$^-$ in RhdA. Performing the analogous reactions with perselenide **2** and thioselenide **3** resulted in immediate conversion to the parent chalcogenates and SeCN$^-$ as evidenced by a new peak in the ^{77}Se NMR spectrum –307.0 ppm and a new IR stretch at 2062 cm^{-1}, both of which corresponding to SeCN$^-$. The enhanced reactivity of terminal selenides **2** and **3** toward CN$^-$ when compared to terminal sulfides **1** and **4** is consistent with the lower reduction potential of Se than S, and this may offer further explanation to the biological utility of RSSe$^-$ in Se-substituted RhdA *in vitro* where detoxification of CN$^-$ by RSSe$^-$ is more facile than RSS$^-$ in S-substituted RhdA.

To investigate whether **1-4** could be trapped with suitable electrophiles, we also treated **1-4** with BnBr and monitored the reactions by ^{1}H NMR spectroscopy. Addition of one equiv. of homodichalcogenide **1** or **2** with BnBr in CD$_3$CN at –35 ºC led to the immediate and quantitative conversion to form Bn$_2$S$_2$ and Bn$_2$Se$_2$, respectively. When performing this reaction with heterodichalcogenides **3** and **4** under similar conditions, we observed formation of the major products Bn$_2$S$_2$ and Bn$_2$Se$_2$ as expected, as well as the minor product BnSSeBn resulting from chalcogen exchange. Similar exchange reactions have been reported previously for RSSeR in the presence of nucleophiles.[48, 49] Overall, the direct electrophilic trapping of **1-4** further confirms that such species behave as discrete dichalcogenides rather than higher order polychalcogenides in solution. Despite the simplicity of such trapping reactions in isolated system, earlier efforts from our group to trap RSS$^-$ generated *in situ* from RSSH led to capture of higher-order organic polysulfides, and recent work by Tsui and coworkers to alkylate a related Zn-bound aryltetrasulfanide only yielded thioethers.[50] In addition to clarifying the stability and reactivity of **1-4** as discrete dichalcogenides in solution, these data also suggest that such species may function as useful synthons to access other dichalcogenide containing small molecules.
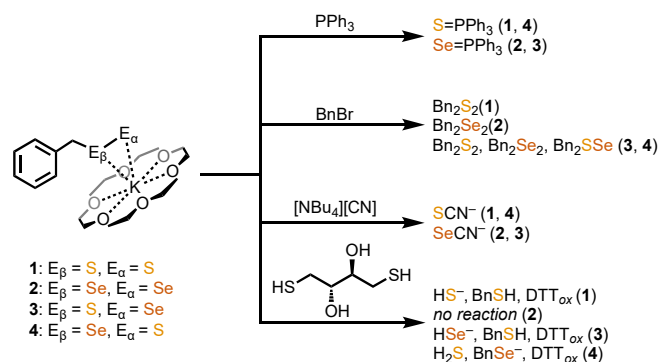
Figure 6. Summary of reactivity of dichalcogenides **1**-**4** toward simple reductants and electrophiles (DTT$_{ox}$: *trans*-4,5-dihydroxy-1,2-dithiane).

Conclusions

We demonstrated that the simple incorporation of contact-ion pairing with [K(18-crown-6)]$^+$ provided a facile route to isolate traditionally elusive dichalcogenide anions and enabled the simple synthesis, characterization, and reactivity of a series of biologically relevant dichalcogenides. Our approach also allowed for the first structural characterization of RSeS$^-$ and RSeSe$^-$ species. In particular, the initial isolation of the highly reactive RSeSe$^-$ perselenide hints reactions between SecSe$^-$ and cellular Se may generate similar reactive intermediates, which could play yet uninvestigated roles in biological Se chemistry, participate in new posttranslational modifications, or contribute to bioselenium signaling pathways. Furthermore, we demonstrated that the isolated dichalcogenides react with reductants like PPh$_3$ and DTT to release reduced chalcogenates and also with [NBu$_4$][CN] to generate SCN$^-$ and SeCN$^-$, which aligns with the proposed reactivity of these motifs in biology. More broadly, in addition to advancing our understanding of these highly reactive dichalcogenide motifs, we anticipate that access to these simple synthons may enable further bio(in)organic investigations into related RSS and RSeS and advance the important roles of S and Se in biology.

Acknowledgements

References

1.   Wang, R., Two's company, three's a crowd: can H_2S be the third endogenous gaseous transmitter? *The FASEB Journal* **2002,** *16* (13), 1792-1798.

2.   Coletta, C.; Papapetropoulos, A.; Erdelyi, K.; Olah, G.; Módis, K.; Panopoulos, P.; Asimakopoulou, A.; Gerö, D.; Sharina, I.; Martin, E.; Szabo, C., Hydrogen sulfide and nitric oxide are mutually dependent in the regulation of angiogenesis and endothelium-dependent vasorelaxation. *Proceedings of the National Academy of Sciences* **2012,** *109* (23), 9161-9166.

3.   Cupp-Sutton, K. A.; Ashby, M. T., Biological Chemistry of Hydrogen Selenide. *Antioxidants* **2016,** *5* (4), 42.

4.   Mertz, W., The Essential Trace Elements. *Science* **1981,** *213* (4514), 1332-1338.

5.   Kayrouz, C. M.; Huang, J.; Hauser, N.; Seyedsayamdost, M. R., Biosynthesis of selenium-containing small molecules in diverse microorganisms. *Nature* **2022,** *610* (7930), 199-204.

6.   Newton, T. D.; Pluth, M. D., Development of a hydrolysis-based small-molecule hydrogen selenide (H_2Se) donor. *Chem. Sci.* **2019,** *10* (46), 10723-10727.

7.   Newton, T. D.; Bolton, S. G.; Garcia, A. C.; Chouinard, J. E.; Golledge, S. L.; Zakharov, L. N.; Pluth, M. D., Hydrolysis-Based Small-Molecule Hydrogen Selenide (H_2Se) Donors for Intracellular H_2Se Delivery. *J. Am. Chem. Soc.* **2021,** *143* (46), 19542-19550.

8.   Hankins, R. A.; Carter, M. E.; Zhu, C.; Chen, C.; Lukesh, J. C., Enol-mediated delivery of H_2Se from γ-keto selenides: mechanistic insight and evaluation. *Chem. Sci.* **2022,** *13* (44), 13094-13099.

9.   Kang, X.; Huang, H.; Jiang, C.; Cheng, L.; Sang, Y.; Cai, X.; Dong, Y.; Sun, L.; Wen, X.; Xi, Z.; Yi, L., Cysteine-Activated Small-Molecule H_2Se Donors Inspired by Synthetic H_2S Donors. *J. Am. Chem. Soc.* **2022,** *144* (9), 3957-3967.

10.   Kong, F.; Ge, L.; Pan, X.; Xu, K.; Liu, X.; Tang, B., A highly selective near-infrared fluorescent probe for imaging H_2Se in living cells and in vivo. *Chem. Sci.* **2016,** *7* (2), 1051-1056.

11.   Kong, F.; Zhao, Y.; Liang, Z.; Liu, X.; Pan, X.; Luan, D.; Xu, K.; Tang, B., Highly Selective Fluorescent Probe for Imaging H_2Se in Living Cells and in Vivo Based on the Disulfide Bond. *Analytical Chemistry* **2017,** *89* (1), 688-693.

12.   Xin, F.; Tian, Y.; Zhang, X., Ratiometric fluorescent probe for highly selective detection of gaseous H_2Se. *Dyes and Pigments* **2020,** *177*, 108274.

13.   Hu, B.; Cheng, R.; Gao, X.; Pan, X.; Kong, F.; Liu, X.; Xu, K.; Tang, B., Targetable Mesoporous Silica Nanoprobes for Mapping the Subcellular Distribution of H2Se in Cancer Cells. *ACS Applied Materials & Interfaces* **2018,** *10* (20), 17345-17351.

14.   Lau, N.; Pluth, M. D., Reactive sulfur species (RSS): persulfides, polysulfides, potential, and problems. *Current Opinion in Chemical Biology* **2019,** *49*, 1-8.

15.   Reich, H. J.; Hondal, R. J., Why Nature Chose Selenium. *ACS Chem. Biol.* **2016,** *11* (4), 821-841.

16.   Mishanina, T. V.; Libiad, M.; Banerjee, R., Biogenesis of reactive sulfur species for signaling by hydrogen sulfide oxidation pathways. *Nat Chem Biol* **2015,** *11* (7), 457-464.

17.   Weekley, C. M.; Harris, H. H., Which form is that? The importance of selenium speciation and metabolism in the prevention and treatment of disease. *Chem. Soc. Rev.* **2013,** *42* (23), 8870-8894.

18.   Stadtman, T. C., Selenium Biochemistry. *Science* **1974,** *183* (4128), 915-922.

19.   Stadtman, T. C., Selenium-Dependent Enzymes. *Annual Review of Biochemistry* **1980,** *49* (1), 93-110.

20.   Filipovic, M. R.; Zivanovic, J.; Alvarez, B.; Banerjee, R., Chemical Biology of H_2S Signaling through Persulfidation. *Chem. Rev.* **2018,** *118* (3), 1253-1337.

21.   Everett, S. A.; Folkes, L. K.; Wardman, P.; Asmus, K. D., Free-Radical Repair by a Novel Perthiol: Reversible Hydrogen Transfer and Perthiyl Radical Formation. *Free Radical Research* **1994,** *20* (6), 387-400.

22.   Braymer, J. J.; Lill, R., Iron–sulfur cluster biogenesis and trafficking in mitochondria. *Journal of Biological Chemistry* **2017,** *292* (31), 12754-12763.

23.   Westley, J., Rhodanese. In *Advances in Enzymology and Related Areas of Molecular Biology*, John Wiley & Sons, Ltd: 1973; pp 327-368.

24.   Nandi, D. L.; Horowitz, P. M.; Westley, J., Rhodanese as a thioredoxin oxidase. *The International Journal of Biochemistry & Cell Biology* **2000,** *32* (4), 465-473.

25.   Ploegman, J. H.; Drent, G.; Kalk, K. H.; Hol, W. G. J.; Heinrikson, R. L.; Keim, P.; Weng, L.; Russell, J., The covalent and tertiary structure of bovine liver rhodanese. *Nature* **1978,** *273* (5658), 124-129.

26.   Kimura, Y.; Koike, S.; Shibuya, N.; Lefer, D.; Ogasawara, Y.; Kimura, H., 3-Mercaptopyruvate sulfurtransferase produces potential redox regulators cysteine- and glutathione-persulfide (Cys-SSH and GSSH) together with signaling molecules H_2S_2, H_2S_3 and H_2S. *Sci Rep* **2017,** *7* (1), 10459.

27.   Ogasawara, Y.; Lacourciere, G.; Stadtman, T. C., Formation of a selenium-substituted rhodanese by reaction with selenite and glutathione: Possible role of a protein perselenide in a selenium delivery system. *Proceedings of the National Academy of Sciences* **2001,** *98* (17), 9494-9498.

28.   Marques, M. C.; Coelho, R.; Pereira, I. A. C.; Matias, P. M., Redox state-dependent changes in the crystal structure of [NiFeSe] hydrogenase from Desulfovibrio vulgaris Hildenborough. *International Journal of Hydrogen Energy* **2013,** *38* (21), 8664-8682.

29.   Mota, C. S.; Rivas, M. G.; Brondino, C. D.; Moura, I.; Moura, J. J. G.; González, P. J.; Cerqueira, N. M. F. S. A., The mechanism of formate oxidation by metal-dependent formate dehydrogenases. *J Biol Inorg Chem* **2011,** *16* (8), 1255-1268.

30.   Bailey, T. S.; Zakharov, L. N.; Pluth, M. D., Understanding Hydrogen Sulfide Storage: Probing Conditions for Sulfide Release from Hydrodisulfides. *J. Am. Chem. Soc.* **2014,** *136* (30), 10573-10576.

31.   Ishii, A.; Takahashi, T.; Tawata, A.; Furukawa, A.; Oshida, H.; Nakayama, J., First synthesis and characterization of isolable thioselenenic acid, triptycene-9-thioselenenic acid. *Chem. Commun.* **2002,** (23), 2810-2811.

32.   Galardon, E.; Tomas, A.; Selkti, M.; Roussel, P.; Artaud, I., Synthesis, Characterization, and Reactivity of Alkyldisulfanido Zinc Complexes. *Inorg. Chem.* **2009,** *48* (13), 5921-5927.

33.   Krautscheid, U.; Dev, S.; Krautscheid, H.; Paul, P. P.; Wilson, S. R.; Rauchfuss, T. B., N-Methylimidazole Mediated Chemistry of Transition Metal Phenylthiolates. The Isolation of the Perthiolate Salts $[M(N\text{-}MeIm)_6](S_2Ph)_2$. *Zeitschrift für Naturforschung B* **1993,** *48* (5), 653-658.

34.   Jungen, S.; Paenurk, E.; Chen, P., Synthesis, Spectroscopic, and Structural Characterization of Organyl Disulfanides and a Tetrasulfanide. *Inorg. Chem.* **2020,** *59* (17), 12322-12336.

35.   Jungen, S.; Chen, P., Synthesis, Isolation, and Characterization of a Phenylsulfane-Selenolate Compound. *Inorg. Chem.* **2020,** *59* (18), 13315-13319.

36.   Schürmann, C. J.; Teuteberg, T. L.; Stückl, A. C.; Ruth, P. N.; Hecker, F.; Herbst-Irmer, R.; Mata, R. A.; Stalke, D., Trapping X-ray Radiation Damage from Homolytic Se−C Bond Cleavage in BnSeSeBn Crystals (Bn=benzyl, $CH_2C_6H_5$). *Angewandte Chemie International Edition* **2022,** *61* (26), e202203665.

37.   Hamsath, A.; Xian, M., Chemistry and Chemical Biology of Selenenyl Sulfides and Thioseleninic Acids. *Antioxidants & Redox Signaling* **2020,** *33* (16), 1143-1157.

38.   Shimada, K.; Goto, K.; Kawashima, T.; Takagi, N.; Choe, Y.-K.; Nagase, S., Isolation of a Se-Nitrososelenol: A New Class of Reactive Nitrogen Species Relevant to Protein Se-Nitrosation. *J. Am. Chem. Soc.* **2004,** *126* (41), 13238-13239.

39.   Goto, K.; Sonoda, D.; Shimada, K.; Sase, S.; Kawashima, T., Modeling of the 5′-Deiodination of Thyroxine by Iodothyronine Deiodinase: Chemical Corroboration of a Selenenyl Iodide Intermediate. *Angewandte Chemie* **2010,** *122* (3), 555-557.

40.   Smiles, D. E.; Wu, G.; Hayton, T. W., Reversible Chalcogen-Atom Transfer to a Terminal Uranium Sulfide. *Inorg. Chem.* **2014,** *53* (24), 12683-12685.

41.   Smiles, D. E.; Wu, G.; Hayton, T. W., Synthesis of Terminal Monochalcogenide and Dichalcogenide Complexes of Uranium Using Polychalcogenides, $[En]^{2-}$ (E = Te, n = 2; E = Se, n = 4), as Chalcogen Atom Transfer Reagents. *Inorg. Chem.* **2014,** *53* (19), 10240-10247.

42.   Hosseininasab, V.; Bertke, J. A.; Warren, T. H., Thionitrite and Perthionitrite in NO Signaling at Zinc. *Angewandte Chemie International Edition* **2021,** *60* (39), 21184-21188.

43.   van Dijk, B.; Visser, G. J., Note on the space group of dibenzyl disulphide. *Acta Crystallographica Section B* **1971,** *27* (4), 846.

44.   Illyés, T.-Z.; Balla, S.; Bényei, A.; Kumar , A. A.; Timári, I.; Kövér, K. E.; Szilágyi, L., Exploring the Syntheses of Novel Glycomimetics. Carbohydrate Derivatives with Se-S- or Se-Se-Glycosidic Linkages. *ChemistrySelect* **2016,** *1* (10), 2383-2388.

45.   du Mont, W.-W.; Mugesh, G.; Wismach, C.; Jones, P. G., Reactions of Organoselenenyl Iodides with Thiouracil Drugs: An Enzyme Mimetic Study on the Inhibition of Iodothyronine Deiodinase. *Angewandte Chemie International Edition* **2001,** *40* (13), 2486-2489.

46.   Figliola, C.; Male, L.; Horton, P. N.; Pitak, M. B.; Coles, S. J.; Horswell, S. L.; Grainger, R. S., [FeFe]-Hydrogenase Synthetic Mimics Based on Peri-Substituted Dichalcogenides. *Organometallics* **2014,** *33* (17), 4449-4460.

47.   Bailey, T. S.; Pluth, M. D., Reactions of isolated persulfides provide insights into the interplay between H2S and persulfide reactivity. *Free Radical Biology and Medicine* **2015,** *89*, 662-667.

48.   Canal-Martín, A.; Pérez-Fernández, R., Biomimetic selenocystine based dynamic combinatorial chemistry for thiol-disulfide exchange. *Nature Communications* **2021,** *12* (1), 163.

49.   Steinmann, D.; Nauser, T.; Koppenol, W. H., Selenium and Sulfur in Exchange Reactions: A Comparative Study. *The Journal of Organic Chemistry* **2010,** *75* (19), 6696-6699.

50.   Seo, W. T. M.; Ballesteros, M., II; Tsui, E. Y., Sulfane Decreases the Nucleophilic Reactivity of Zinc Thiolates: Implications for Biological Reactive Sulfur Species. *J. Am. Chem. Soc.* **2022,** *144* (45), 20630-20640.